Journal of the Meteorological Society of Japan, Vol. 73, No. 6, pp. 975–991, 1995

Sensitivity of the GCM-Simulated Large-Scale Structures to Two Cumulus Parameterizations

By Jong-Jin Baik[1,2] and Masaaki Takahashi

Center for Climate System Research, University of Tokyo, Tokyo 153, Japan

(Manuscript received 22 December 1994, in revised form 14 July 1995)

Abstract

To examine the sensitivity of the simulated large-scale structures to the Betts-Miller and the Arakawa-Schubert cumulus parameterizations, a series of 6-month integrations are performed using the CCSR/NIES atmospheric general circulation model with a horizontal triangular resolution of 21 and 20 vertical levels. The model results are time-averaged for the last three months, that is, June-July-August mean. Comparisons between the simulations using the Betts-Miiler scheme and the Arakawa-Schubert scheme indicate that although the simulated large-scale structures are generally similar to each other, there are some noticeable differences. These include the temperatures in the middle and upper troposphere at mid-latitudes in the northern hemisphere, the location of the maximum convective heating in the tropical deep convective region, the convective heating/cooling in the boundary layer, the precipitation distribution pattern over the tropical western Pacific and the vertical profile of the vertical turbulent heat transport. Sensitivity experiments with different adjustment parameters in the Betts-Miller scheme show that the precipitation distribution pattern over the tropical western Pacific is very sensitive to the adjustment time scale and stability weight as well as the saturation pressure departure. It is also shown that the partition between the convective precipitation and the large-scale precipitation is most sensitive to the saturation pressure departure.

1. Introduction

Cumulus convection plays an important role in determining the large-scale thermodynamic and dynamic state of the atmosphere and, hence, in maintaining the general circulation and climate. It affects the large-scale flow through diabatic heating due to latent heat release, vertical turbulent transports of heat, moisture and momentum and interaction with radiation (Tiedtke, 1988). In large-scale models, cumulus convection is essentially subgrid-scale process and the collective effects of the nonresolvable convective process on the grid-scale should be properly represented in terms of the resolvable fields with some closure assumptions. Cumulus parameterization schemes used in large-scale models can be categorized into three groups: the moist convective adjustment scheme (Manabe *et al.*, 1965; Betts, 1986; Betts and Miller, 1993), the moisture convergence scheme (Kuo, 1965, 1974; Anthes, 1977) and the mass-flux scheme (Arakawa and Schubert, 1974; Tiedtke, 1989; Hack, 1994).

The basic idea behind moist convective adjustment schemes is that in the presence of cumulus convection the local thermodynamic structure is constrained by convection and adjusted toward a quasi-equilibrium reference state. The scheme proposed by Manabe *et al.* (1965) relaxes the thermodynamic profiles toward a moist adiabat. This scheme has been successfully used in general circulation models (GCMs) such as the GFDL GCM (*e.g.*, Manabe and Hahn, 1981) and the NCAR community climate model (CCM) (*e.g.*, Pitcher *et al.*, 1983) [Recently, the CCM replaced the moist adiabatic adjustment scheme by a stability-dependent mass-flux scheme (Hack, 1994)]. On the other hand, the scheme proposed by Betts (1986) and improved by Betts and Miller (1993) relaxes the thermodynamic profiles toward an observed quasi-equilibrium state with an adjustment time scale. Since the observed quasi-equilibrium thermodynamic structure in tropical convective regions differs much from the moist adiabatic reference state (Betts, 1986), the use of

1 On leave from Global Environment Laboratory, Yonsei University, Seoul, Korea

2 Present affiliation: Department of Environmental Science and Engineering, Kwangju Institute of Science and Technology, Kwangju, Korea

observed reference profiles seems to be more appropriate.

The Betts-Miller scheme has been tested and evaluated in many numerical models. The test of the scheme in the ECMWF global forecast model, in comparison with the Kuo scheme, shows some improvement in the tropical mean flow (Betts and Miller, 1986) and better vertical consistency between the divergent circulation and vertical velocity fields in tropical cyclone forecast experiments (Puri and Miller, 1990). Baik *et al.* (1990b) showed through tropical cyclone simulations that the convective adjustment parameters in the scheme influence the grid-scale precipitation as well as the convective precipitation and the precipitation is particularly sensitive to changes in the saturation pressure departure. The high sensitivity of the simulated precipitation to the saturation pressure departure was also confirmed by Alapaty *et al.* (1994) in a numerical study of orographic-convective rainfall during the Indian southwest monsoon using a limited-area nested model. The scheme is also implemented into the eta-model of the U.S. NMC (Janjić, 1990, 1994) and the CSIRO limited-area model of Australia (Evans *et al.*, 1994).

However, the above-mentioned studies using the Betts-Miller scheme are limited to relatively short-time integrations because of the constraint of limited-area or forecast models. In addition, the cumulus parameterization scheme is best suited and tested for models with a coarse horizontal resolution such as GCMs because the quasi-equilibrium assumption may be valid only for slowly varying fields, but not for fast varying systems (Tiedtke, 1988). The performance of the Betts-Miller scheme in a long-term simulation is yet to be evaluated.

There are many numerical studies which examine the sensitivity of simulated climate to cumulus parameterizations. Albrecht *et al.* (1986) found that a hybrid cumulus parameterization scheme with the convective moisture and heat transports results in the higher upper-tropospheric temperature and the greater tropospheric water vapor content than the moist adiabatic adjustment scheme. In the CO_2 sensitivity experiments with sea surface temperature uniformly increased, Cunnington and Mitchell (1990) showed that the penetrative convection scheme (Slingo *et al.*, 1989) gives the greater warming and the larger reduction in cloud in the upper tropical troposphere than the layer-swapping convective adjustment scheme. Hack (1994) found that in contrast to the moist adiabatic adjustment scheme the stability-dependent mass-flux scheme significantly warms and moistens the troposphere, particularly in the tropics. These studies indicate large differences between simulated climates using the mass-flux scheme, which effectively transports moisture upward, and the moist adiabatic adjustment scheme. Tiedtke (1988) presented the role of model penetrative cumulus convection by comparing simulations which use different cumulus parameterizations.

In this paper, we extend previous studies to investigate the sensitivity of simulated large-scale structures to two cumulus parameterization schemes, that is, the Arakawa-Schubert scheme and the Betts-Miller scheme and to adjustment parameters in the Betts-Miller scheme. For this purpose, the Betts-Miller scheme is first implemented into the CCSR/NIES (Center for Climate System Research/National Institute for Environmental Studies) GCM. Then, a series of 6-month integrations are performed with each cumulus parameterization and different adjustment parameters and the simulations are compared. A description of the numerical model and the subgrid-scale cumulus parameterizations are given in section 2 and section 3, respectively. In section 4, simulation results with different cumulus parameterization schemes are intercompared and discussed. Also, results of the sensitivity to adjustment parameters are presented. Conclusion is given in the last section.

2. Model description

The CCSR/NIES spectral atmospheric general circulation model has been developed at the Center for Climate System Research, University of Tokyo, and the National Institute for Environmental Studies (Numaguti, 1993; Numaguti *et al.*, 1994) and has been used to study the Hadley circulation and tropical precipitation (Numaguti, 1993), the QBO-like oscillation in a 2-dimensional version (Takahashi, 1993) *etc.* The model used in this study is the test version 5.3 of the CCSR/NIES GCM, which is summarized in Table 1. For the present study, the large-scale cloud process with a prognostic equation for cloud liquid water content and the large-scale cloud microphysics is replaced by a simple diagnostic large-scale condensation process and the radiation scheme of Nakajima and Tanaka (1986) is replaced by the Chou's radiation scheme (*e.g.*, Chou, 1992). The diagnostic large-scale condensation scheme is chosen simply because the horizontal resolution in the present experiments appears to be coarse ($T21$) for the explicit large-scale cloud microphysics, although the prognostic cloud scheme is expected to give relatively accurate information for an interactive cloud-radiation process which is known to play an important role in a climate modeling. The Chou's radiation scheme is chosen because we have learned through the extensive numerical experiments that this scheme produces smoother temperature distribution field in the stratosphere than the present standard version of the radiation scheme. However, the CCSR/NIES radiation scheme already underwent a minor change in its adaptation to the

Table 1. A summary of the test version 5.3 of the CCSR/NIES atmospheric general circulation model (standard case) [based on Numaguti and Kumakura (1994)].

equation system	primitive equation system
prognostic variables	surface pressure, vorticity, divergence, temperature, water vapor specific humidity, cloud liquid water content
horizontal discretization	spectral method (triangular truncation)
vertical discretization	σ system (Arakawa and Suarez, 1983)
time discretization	semi-implicit scheme, leap-frog scheme
radiation	2 stream DOM/adding method (Nakajima and Tanaka, 1986)
large-scale cloud process	prognostic cloud liquid water content (Le Treut and Li, 1991)
subgrid-scale cumulus convection	Arakawa-Schubert (1974) scheme with convective downdrafts and prognostic cloud base mass-flux
vertical diffusion	Mellor and Yamada (1974, 1982) level 2 scheme nonlocal diffusion of convective mixed layer
surface flux	Louis (1979) bulk formula convective effect (Miller *et al.*, 1992)
ground process	multi-layer thermal conduction new bucket model (Kondo, 1993)
gravity-wave drag	McFarlane (1987)

GCM to better simulate climate in the stratosphere at the time of writing this paper (A. Numaguti, 1994, personal communication).

The experiments are performed with a horizontal triangular resolution of 21 ($T21 \sim 5.6° \times 5.6°$ transform grid), 20 vertical levels (14 levels between $\sigma = 1$ and 0.1 and 6 levels between $\sigma = 0.1$ and 0) and a time step of 30 min. Starting from 1 January with the idealized initial conditions, the model is integrated for 14 months for the model's spinup. The model integration is interrupted on 1 March of the second year and the data at the final time step are saved. Then, each cumulus parameterization experiment is activated and the model is integrated for 6 months (from 1 March to 31 August) using the saved data as initial conditions. All the results presented in this paper are the time averages of the last three months, that is, June, July and August (northern hemisphere summer season). Note that both the 14-month and 6-month integrations include diurnal and seasonal cycles. The sea surface temperatures are specified using the climatological monthly mean values. Our concern in this study is to intercompare the large-scale structures simulated using the different cumulus parameterizations and convective adjustment parameters rather than to compare the simulation fields with observations since 6-month integration seems to be not long enough to produce a quasi-steady climate.

3. Subgrid-scale cumulus parameterizations

The CCSR/NIES GCM contains the Arakawa-Schubert scheme as a standard one as shown in Table 1 and for this study the Betts-Miller scheme is implemented into the model. A brief description of each cumulus parameterization scheme is given below.

The Arakawa-Schubert scheme (AS scheme hereafter) describes the mutual interaction of a cumulus cloud ensemble with the large-scale environment and employs a quasi-equilibrium hypothesis which expresses a balance between the generation of moist convective instability by large-scale processes and its destruction by cumulus convection. The scheme is applied to a conditionally unstable atmosphere. All the subensemble clouds are assumed to have same cloud base. The effects of convective downdrafts are included because the original scheme without them tends to produce the excessive warming and drying in the lower troposphere (Cheng and Arakawa, 1990). The cloud base mass-flux is predicted with a constraint of its non-negative value rather than diagnostically determined using, say, the simplex linear algorithm. The precipitation efficiency in the cumulus model is assumed to be an exponential function of height.

The Betts-Miller scheme (BM scheme hereafter) allows for nonprecipitating shallow convection as well as precipitating deep convection. The deep convection scheme accounts for the observed fact that the thermal structure below the freezing level is more unstable than the moist adiabat with a maximum subsaturation (in magnitude) near the freezing level. On the other hand, the shallow convection scheme is based on the observed fact that the thermodynamic structure in the shallow convective regions tends to follow a mixing line that connects the saturation point of air above the cloud layer and that of subcloud air. Convection takes place in a conditionally unstable atmosphere. In this study, a version of the Betts-Miller scheme used by Baik *et al.* (1990a) is utilized. However, the shallow con-

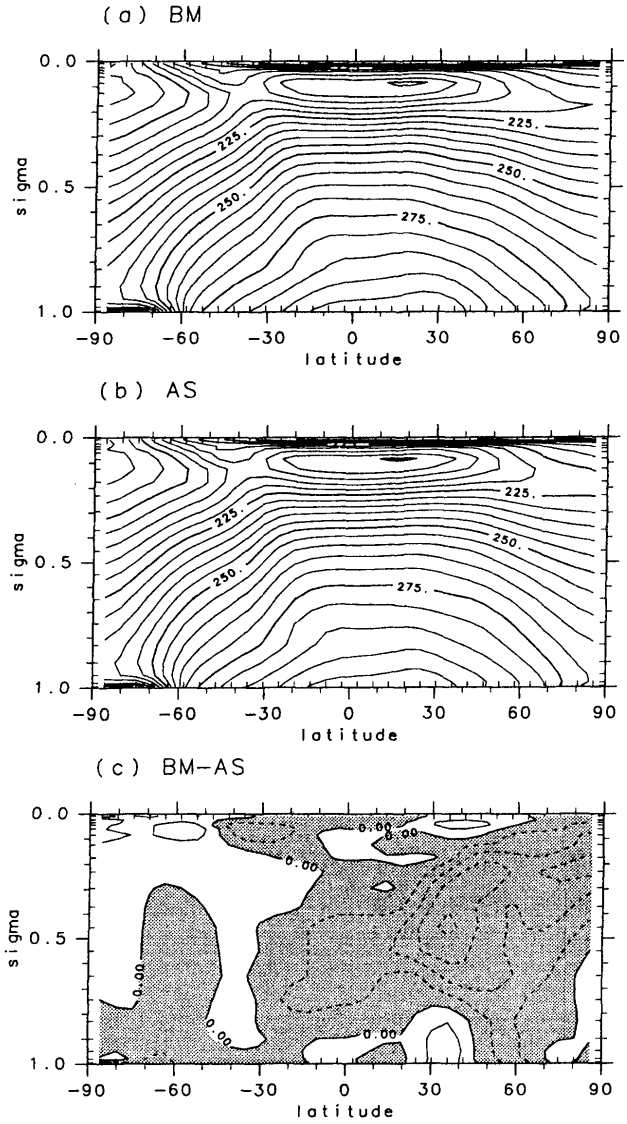

Fig. 1. Zonally-averaged temperature (in K) simulated with (a) the Betts-Miller scheme and (b) the Arakawa-Schubert scheme and (c) difference between the zonally-averaged temperatures simulated with the two schemes (BM minus AS). Contour interval is 5°C in (a) and (b) and 1°C in (c) and the regions with negative values in (c) are shaded.

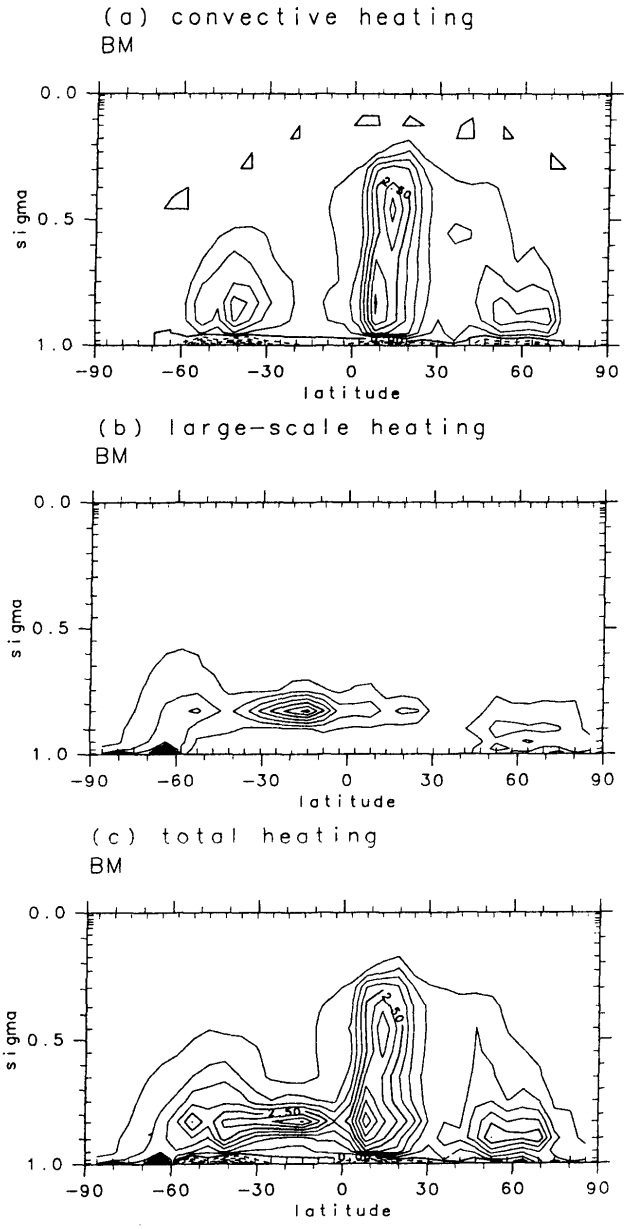

Fig. 2. Zonally-averaged (a) subgrid-scale convective, (b) large-scale and (c) total heating rates (in °C d^{-1}) simulated with the Betts-Miller scheme. Contour interval is 0.5°C d^{-1}.

vection scheme is turned off in this study. This is because we found that the magnitude and vertical shape of shallow convective heating and moistening rates are sometimes unrealistic. Our analysis indicates that this is related to the swap points of the forced shallow cloud top when the deep convection scheme fails to produce positive precipitation, the relatively thick layers just above the determined shallow cloud top height (see the model σ-level configuration shown in figures below), hence misrepresenting mixing line slope, and so on. Further research is needed to modify or improve the shallow convection scheme (Janjić, 1994) to be adapted well in the GCM. For the control simulation (section 4a), the adjustment time scale, the stability weight on the moist adiabat below the freezing level and the saturation pressure departure at the lowest model prediction level are specified as 2 hours, 0.8 and −30 mb, respectively. The sensitivity of the model to the adjustment parameters will be examined in section 4b. The computing time required for the simulation with the AS scheme is almost the same

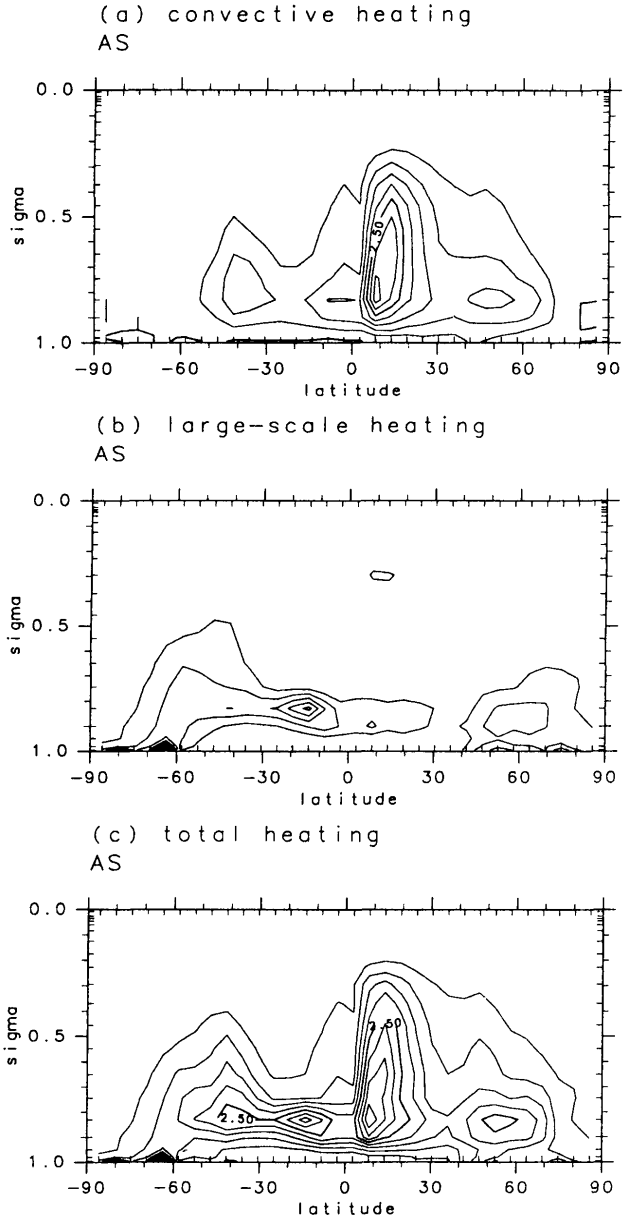

Fig. 3. Zonally-averaged (a) subgrid-scale convective, (b) large-scale and (c) total heating rates (in °C d^{-1}) simulated with the Arakawa-Schubert scheme. Contour interval is 0.5°C d^{-1}.

as that with the BM scheme.

4. Results and discussion

a. *Comparisons between the Betts-Miller scheme and the Arakawa-Schubert scheme*

The zonally-averaged temperatures obtained using the Betts-Miller scheme and the Arakawa-Schubert scheme are shown in Fig. 1, together with the temperature difference between the two cumulus parameterizations. The 15 inner marks on the σ-axis in the latitude-altitude cross sections represent sigma levels on which the wind, temperature and specific humidity are predicted. In both the simulations, the warmest region in the tropical lower troposphere is shifted toward the northern hemisphere as should be expected. Also, both the simulations exhibit a prominent temperature inversion near the surface in the winter polar region, which appears to be too strong compared with other studies (*e.g.*, Pitcher *et al.*, 1983). The zonally-averaged temperature difference field indicates that the AS scheme as a whole produces a warmer tendency northward of ~30°S. The temperature difference is small over the tropics and in the southern hemisphere, but pronounced especially in the middle and upper troposphere at mid-latitudes in the northern hemisphere. In this region, the temperatures in the AS simulation are as much as 4°C higher than those in the BM simulation.

Figures 2 and 3 shows the zonally-averaged convective, large-scale (stable) and total (convective plus large-scale) heating rates for the BM and AS experiments, respectively. In the convective heating fields, although both the schemes simulate similar features of the deep-layer convective heating region associated with intertropical convergence zones and the relatively shallow-layer convective heating regions off the tropics in both hemispheres, there are some differences between the two experiments. In the upper tropical troposphere, the convective heating rate is slightly higher in the BM simulation than in the AS simulation. In the tropical deep convection region, the BM simulation exhibits double maximum convective heating zones in the vertical, one located in the lower troposphere and the other slightly above the mid-troposphere, and the axis connecting these two maximum zones is tilted with the lower maximum situated equatorward. On the other hand, the AS simulation exhibits a single maximum zone located in the lower troposphere. These characteristics are also reflected in the total heating fields. The relatively shallow-layer convection in the southern hemisphere is more intense in the BM experiment than in the AS experiment. Between ~30°N and ~40°N, the AS scheme produces higher convective heating than the BM scheme, partly contributing to the warmer temperature tendency in this region in the AS simulation as shown in Fig. 1c. In the BM simulation, noticeable convective cooling in the boundary layer is observed in association with the convective activity regions. This is present because the Betts-Miller scheme adjusts from below the cloud base level to simulate the effect of cold unsaturated downdrafts (Betts, 1986).

In the grid-scale condensation scheme employed in the present GCM, when the grid-scale supersaturation is found, excess water vapor is condensed to liquid water and latent heat is released (large-scale condensational heating). The liquid water is assumed

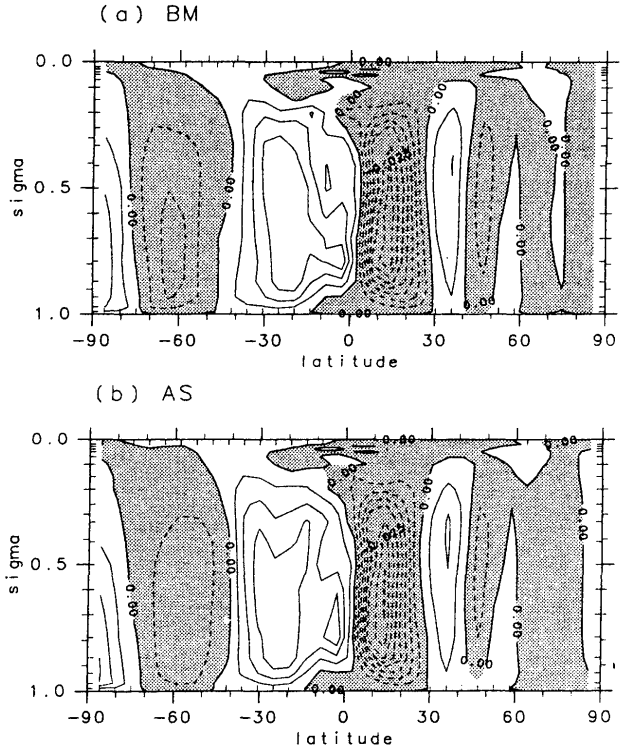

Fig. 4. Zonally-averaged vertical σ-velocity (in d^{-1}) simulated with (a) the Betts-Miller scheme and (b) the Arakawa-Schubert scheme. The contour interval is 0.005 d^{-1} and negative values (upward motion) is shaded.

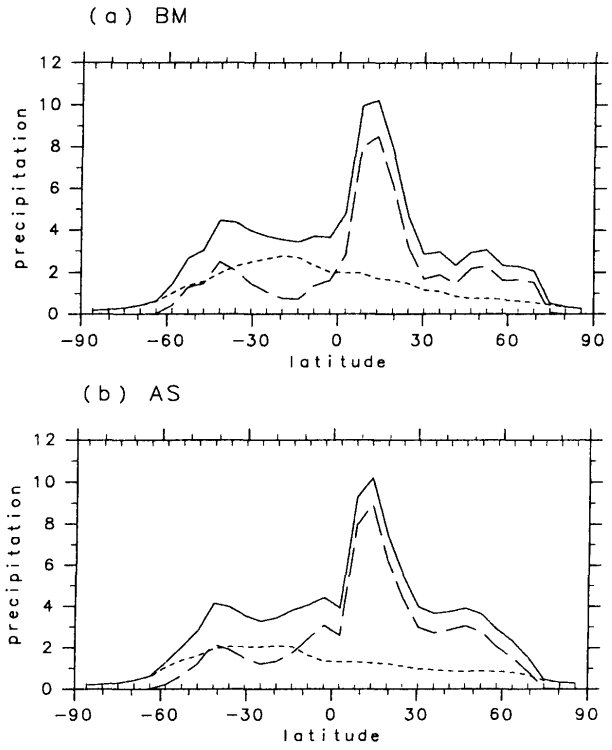

Fig. 5. Zonally-averaged subgrid-scale convective (long-dashed line), large-scale (short-dashed line) and total (solid line) precipitation rates (in mm d^{-1}) simulated with (a) the Betts-Miller scheme and (b) the Arakawa-Schubert scheme.

to immediately fall as rain without evaporation in the air column below. The large-scale heating structures resemble each other and the large-scale heating is confined mainly in the lower troposphere with a concentrated region around 15°S in both the experiments. In this region, the large-scale heating is more intense in the BM experiment than in the AS experiment.

Shallow convection in the tradewind regions plays an important role in maintaining the thermal structure of the lower troposphere and also has a significant influence on the atmospheric energetics by enhancing the hydrological cycle (Tiedtke, 1989). It transports and redistributes heat and moisture in the vertical and the tradewind inversion layer is maintained by the cooling and moistening due to the evaporation of cloud liquid water, which is counteracted by the heating and drying due to the large-scale subsidence. In the present study, the shallow convection in the BM scheme is turned off. Around 15°S, the evaporation from the ocean is large and exceeds the precipitation. Turbulent process is acting to transport moisture upward and can make the lower troposphere supersaturated if the shallow convection is not functioning. It is believed that the absence of the shallow convection process is responsible for the larger large-scale heating in the BM scheme in this region (Fig. 2b). Indeed, an experiment with both the deep and shallow convection schemes, although needed to refine the shallow convection scheme as mentioned in the section 3, showed a nearly absent feature of the concentrated large-scale heating in this region. Interestingly, in the subtropical and tropical regions the simulated large-scale heating field using the stability-dependent mass-flux scheme exhibits negligible large-scale heating rates, but that using the moist adiabatic adjustment scheme exhibits concentrated and elongated large-scale heating zone in the lower troposphere (Hack, 1994). The degree of the performance of the AS scheme in simulating shallow convection, particularly the tradewind shallow cumuli, is not clearly known. Further investigation is required to examine to what extent the concentrated large-scale heating in the lower troposphere around 15°S in the AS scheme (Fig. 3b) is related to the shallow convection and to what degree the AS scheme in the CCSR/NIES GCM simulates the tradewind cumuli.

Figure 4 shows the zonally-averaged vertical σ-velocity for the BM and AS experiments. The mag-

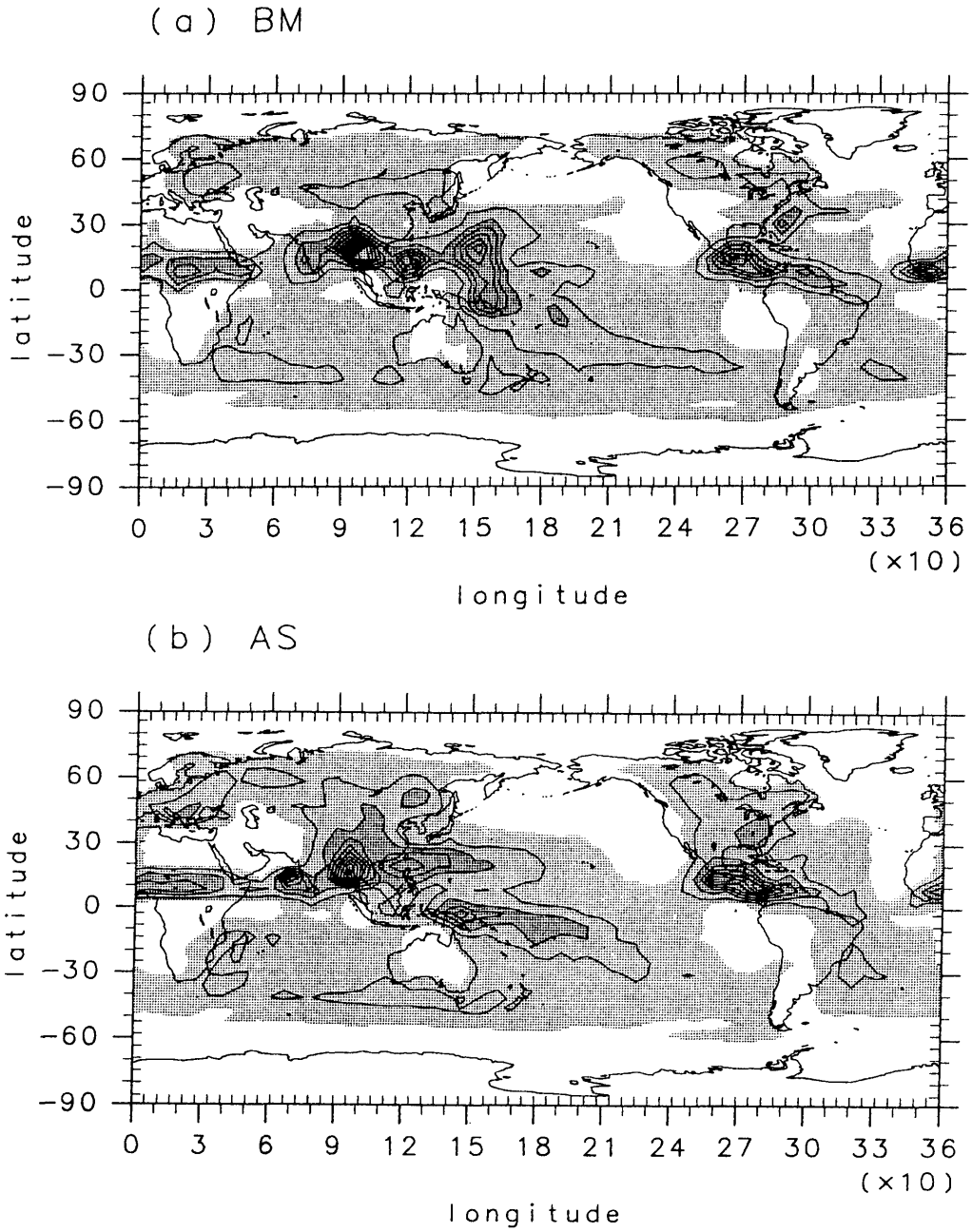

Fig. 6. Geographical distribution of the total precipitation rate (in mm d^{-1}) simulated with (a) the Betts-Miller scheme and (b) the Arakawa-Schubert scheme. Contour interval is 5 mm d^{-1} and the regions with values between 2 and 10 and in excess of 10 are light-shaded and heavy-shaded, respectively. The same contour interval and shading are used in Figs. 9, 11 and 13.

nitude and structure of the vertical velocities are similar to each other. The strong upward motion associated with the tropical deep convection and the subsidence just outside it are well defined. The stronger and wider subtropical subsidence in the southern hemisphere than the corresponding subsidence in the northern hemisphere tends to suppress deep convective activities in this region as can be seen in the convective heating fields (Figs. 2a and 3a).

Figure 5 shows the zonally-averaged convective, large-scale (stable) and total precipitation rates for the BM and AS experiments. The overall pattern of the total precipitation resembles each other, but at middle and high latitudes in the northern hemisphere the total precipitation rate is higher in the AS simulation than in the BM simulation due to the higher convective precipitation over land areas in the AS simulation (see Fig. 6). Over the tropical deep convection region, the total precipitation in both the

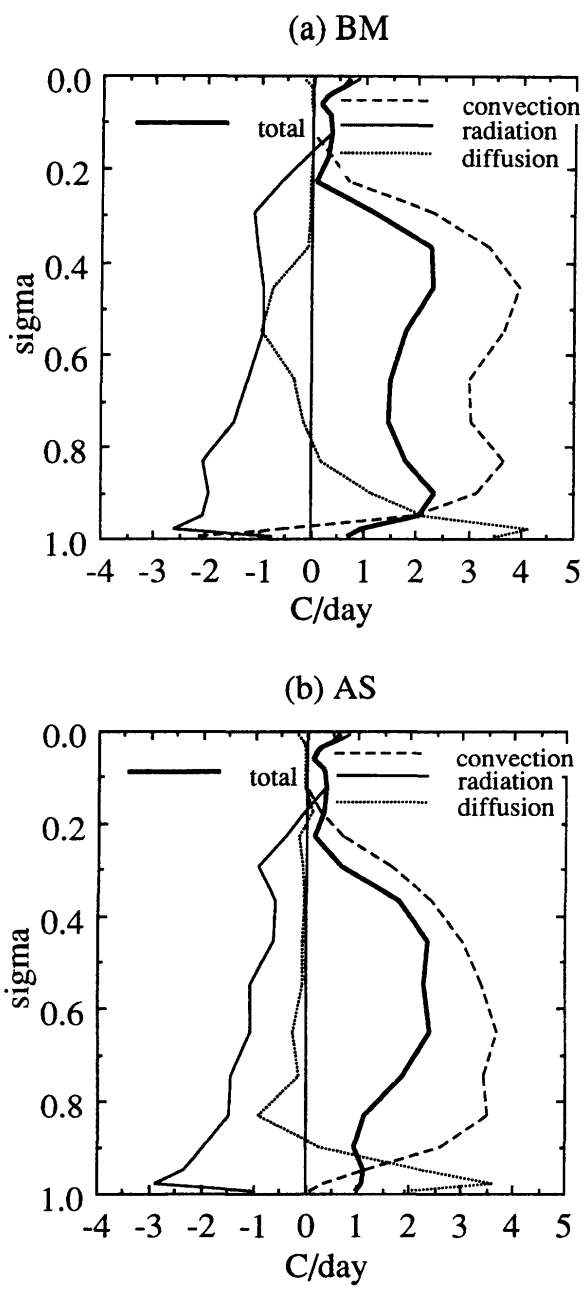

Fig. 7. Vertical profiles of the zonally-averaged various diabatic heat sources (°C d^{-1}) at 13.8°N simulated with (a) the Betts-Miller scheme and (b) the Arakawa-Schubert scheme. The dashed, thin solid, dotted and thick solid lines represent contributions from convection, radiation, diffusion and total, respectively.

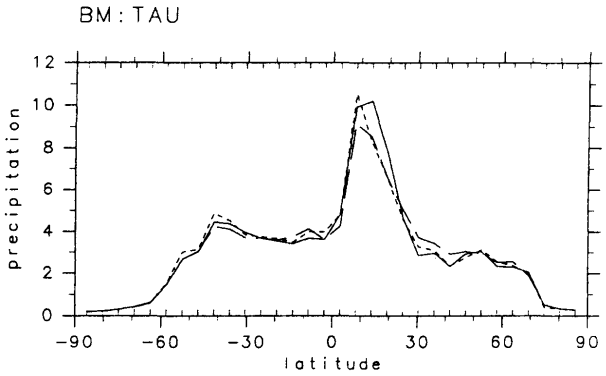

Fig. 8. Zonally-averaged total precipitation rate (in mm d^{-1}) for the sensitivity experiments with different adjustment time scales in the Betts-Miller scheme. The short-dashed, solid and long-dashed lines correspond to τ = 1, 2 and 3 h, respectively.

experiments is mainly contributed by the cumulus parameterization. This is consistent with the result using the stability-dependent mass-flux scheme, but different from the result using the moist adiabatic adjustment scheme which shows a more equal partition between convective and stable precipitations in the tropics (*e.g.*, Hack, 1994). Figure 5 indicates that in the tropical deep convection the partition of the total precipitation into the large-scale precipitation is slightly higher in the BM simulation than in the AS simulation. In the southern flank of the tropical deep convection where the subtropical subsidence exists (Fig. 4), the BM scheme leads to more suppressed convective precipitation, but larger large-scale precipitation than the AS scheme, possibly due to the absence of the shallow convection scheme.

The geographical distribution of the precipitation rate for the BM and AS experiments is illustrated in Fig. 6. The major features of the precipitation distribution are simulated similarly over Central Africa, Central America and the Bay of Bengal and Burma, although the intensity of the precipitation somewhat differs. However, there are some significant differences between the two cumulus parameterizations. Over the tropical western Pacific, the BM simulation shows a concentrated precipitation zone centered around the Philippine Islands and another concentrated broad area that extends northsouthward with some longitudinal extension between ~140°E and ~170°E. On the other hand, the AS simulation shows two zonally-elongated zones of concentrated precipitation, one located near the equator and extending toward the central Pacific and the other at ~20°N. This split of the precipitation zones is to some extent related to the small evaporation efficiency of rain in the cumulus model of the AS scheme (Numaguti *et al.*, 1994). In association with the Indian southwest monsoon, the AS experiment simulates more precipitation over the Arabian sea with its maximum situated off the western Indian coast along which the western Ghats mountains are located than the BM experiment.

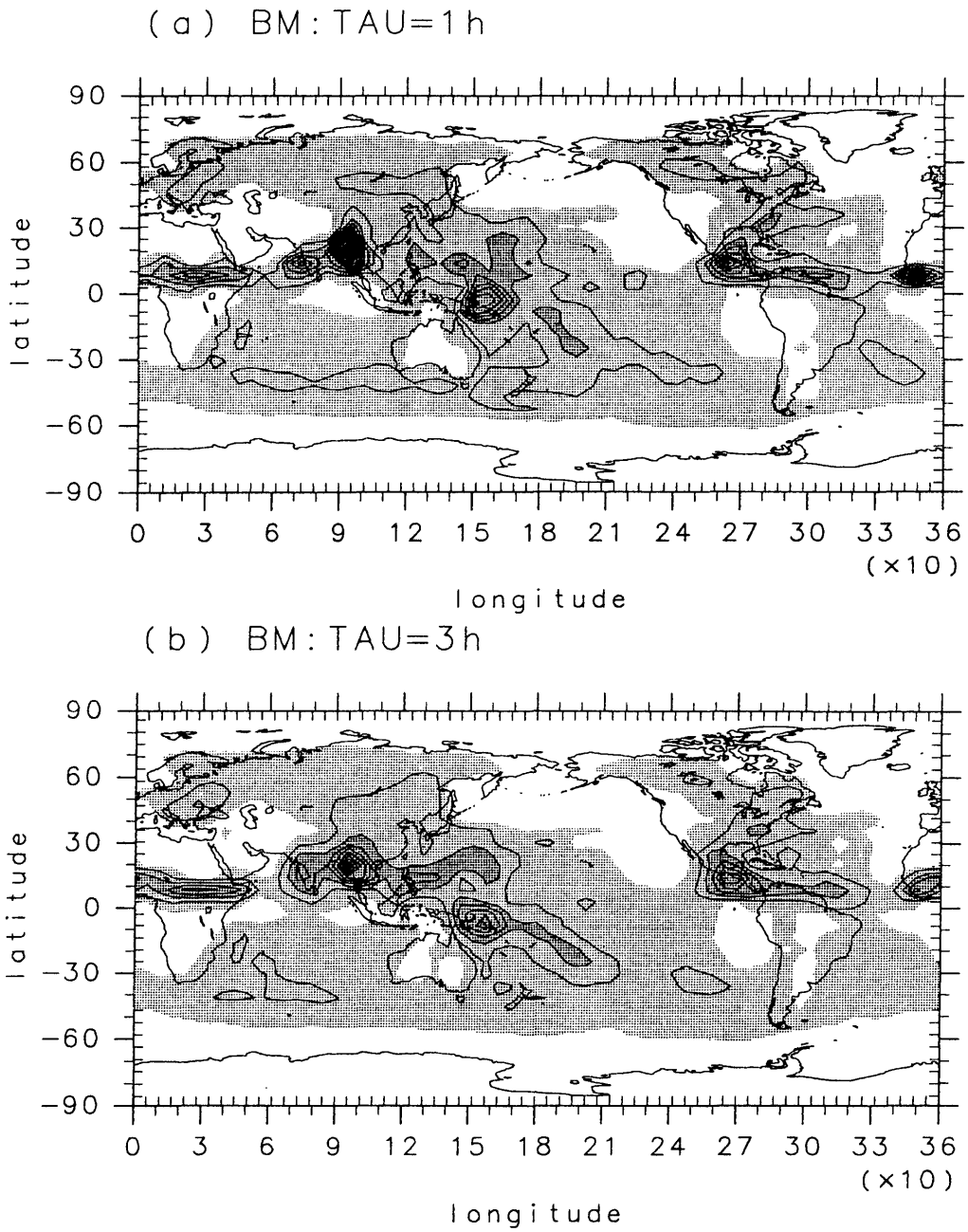

Fig. 9. Geographical distribution of the total precipitation rate (in mm d^{-1}) for the sensitivity experiments with different adjustment time scales in the Betts-Miller scheme: (a) $\tau = 1$ h and (b) $\tau = 3$ h.

The precipitation rate in the AS experiment generally tends to be higher over land areas in the northern hemisphere off the equatorial regions, especially over the Tibetan plateau and North America, than that in the BM experiment.

To examine and compare various diabatic heat sources in active convective regions produced by the two cumulus parameterizations, the vertical profiles of diabatic heatings due to convection, radiation and diffusion processes are plotted in Fig. 7. These are zonally-averaged at 13.8°N, where the zonally-averaged precipitation rate in each experiment, hence the convective activity, is highest as displayed in Fig. 5. The convection in this figure includes contributions from the subgrid-scale convective heating and large-scale condensational heating. The radiation includes contributions from the shortwave and longwave radiative processes. The diffusion includes contributions from the turbulent diffusion process and dry convective adjustment. It was notified in both the experiments that at the lowest model prediction level ($\sigma = 0.995$) the largest

diabatic heating comes from the turbulent diffusion process and the largest cooling comes from the dry convective adjustment.

In the BM simulation, the convection dominates the total diabatic heating. At the lowest levels, the convection cools atmosphere as already explained above and there are double convection maximum zones centered at $\sigma\sim0.83$ and 0.45. This double maximum feature is also manifested in the total diabatic heating profile because of the dominance of the convection contribution. The radiation cools troposphere and heats stratosphere. The diffusion acts to heat the atmosphere below $\sigma\sim0.79$ and cool the layers between $\sigma\sim0.79$ and $\sigma\sim0.35$. In the AS simulation, the total diabatic heating is also dominated by the convection, but the diabatic heating structures are moderately different from those in the BM simulation except for the radiation profile. The convection profile tends to exhibit a broad single convection maximum zone between $\sigma\sim0.83$ and $\sigma\sim0.65$. It is very interesting to note that the vertical extension of the diffusional heating and cooling is shallower in the AS scheme than in the BM scheme. The diffusion process heats the atmosphere below $\sigma\sim0.88$ and cools the atmosphere above it. But, the diffusional cooling rate becomes very small above $\sigma\sim0.74$. The higher vertical extension of the diffusion process in the BM scheme is probably believed to be related to the nonexistence of shallow convection.

A careful examination of the observational data presented by Betts (1986) reveals that in the deep moist convective regions the quasi-equilibrium temperature profiles appear to be a rather steady characteristic, but the moisture profiles are much variable. This evidence strongly suggests that different convective regimes have different quasi-equilibrium thermodynamic structures, especially for the moisture structures. Although convective adjustment parameters in the Betts-Miller scheme may be tuned to yield reasonable results for simulation in a particular convective regime using a limited-area model (*e.g.*, southwest monsoon rainfall simulation by Alapaty *et al.*, 1994), it cannot be expected that any specified reference moisture profile will universally work well for different convective regimes (during evolution as well as in locality), which are always present in the atmosphere of the GCM. Moreover, it cannot be expected that with the specified reference moisture profile the realistic maintenance of the very long-term moisture structure will be established, which is a crucial factor in a climate modeling. This can be considered as a drawback of the BM scheme in a climate modeling, although the scheme has shown a remarkable skill in forecasting the precipitation and storm systems in the limited-area eta-model (Janjić, 1994). Indeed, the most sensitiveness of simulated precipitation to the saturation pressure departure, which will be presented in the next subsection, explains this point to some extent. On the other hand, a determination of moisture content in the Arakawa-Schubert scheme is not constrained by any specification as in the Betts-Miller scheme, but is connected with a spectral cumulus model. Accordingly, in a climate modeling the very long-term moisture structure, in principle, can be reasonably well maintained compared with the BM scheme, provided that the spectral cumulus model collectively well treats some essential physical processes associated with cumulus clouds.

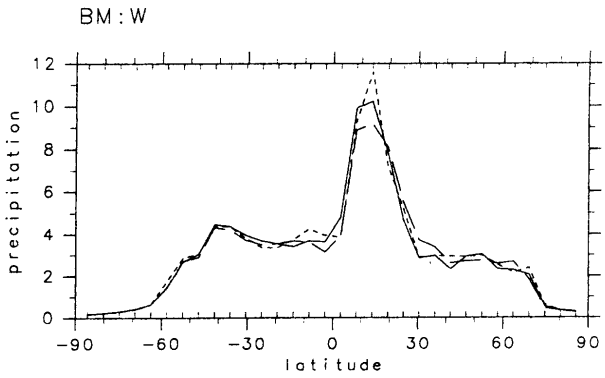

Fig. 10. Zonally-averaged total precipitation rate (in mm d^{-1}) for the sensitivity experiments with different stability weights on the moist adiabat below the freezing level in the Betts-Miller scheme. The short-dashed, solid and long-dashed lines correspond to $w = 0.7$, 0.8 and 0.9, respectively.

b. Sensitivity to adjustment parameters in the Betts-Miller scheme

In this subsection, the sensitivity of the large-scale structures to three convective adjustment parameters in the Betts-Miller scheme (adjustment time scale, stability weight and saturation pressure departure) is investigated. For the sensitivity experiments, each value is varied with the other two held constant.

The convective heating and moistening due to subgrid-scale cumulus convection are given by

$$F_T = \frac{T_{ref} - \bar{T}}{\tau}, \tag{1}$$

$$F_q = \frac{q_{ref} - \bar{q}}{\tau}, \tag{2}$$

respectively. Here, T_{ref} and q_{ref} denote the reference temperature and specific humidity and $\bar{T}$ and $\bar{q}$ denote the grid-point temperature and specific humidity before the convection scheme is applied. The parameter τ is called the adjustment time scale or relaxation time scale which represents the lag between the changing large-scale field and the convective response toward a quasi-equilibrium thermodynamic state (Betts, 1986). When the adjustment

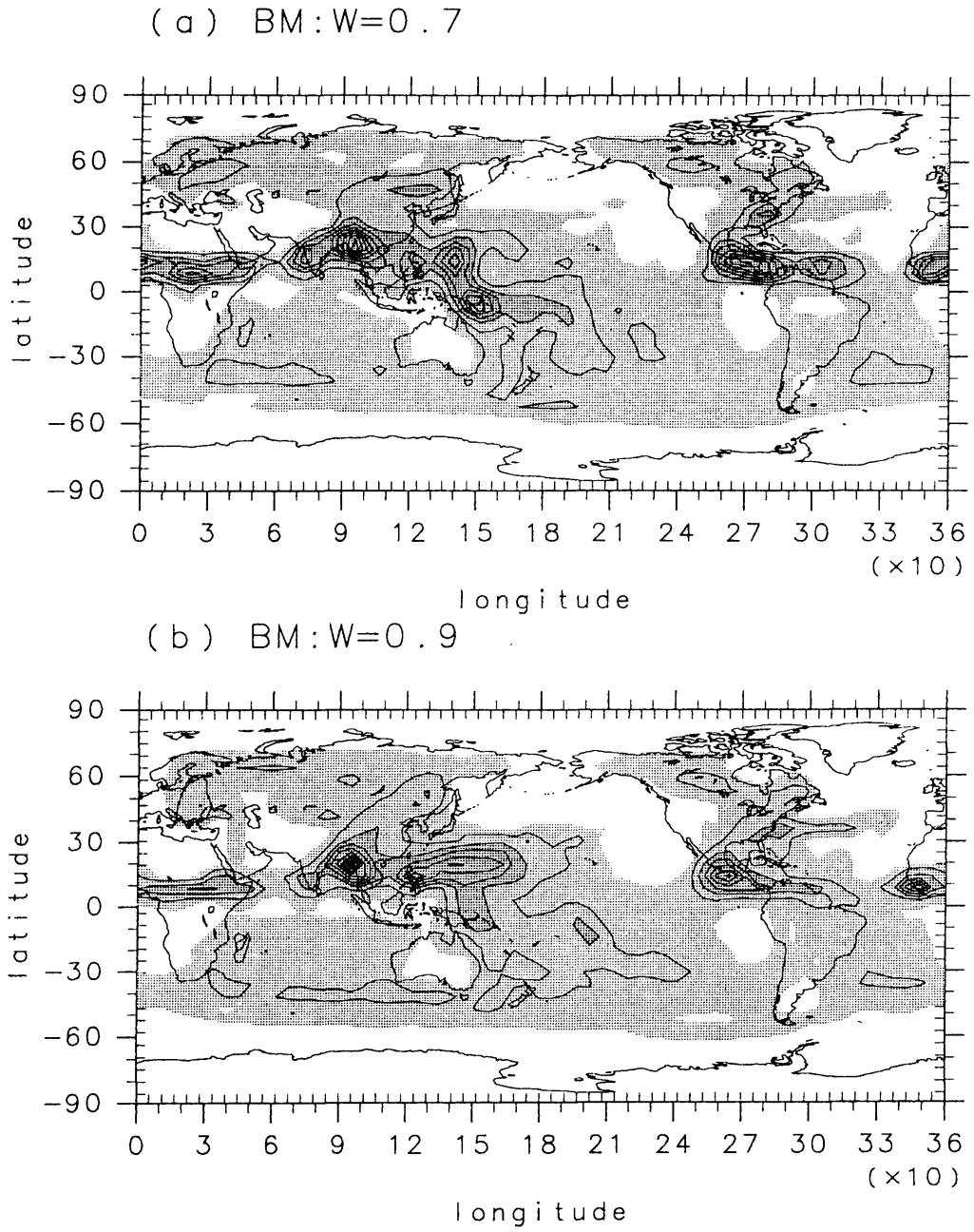

Fig. 11. Geographical distribution of the total precipitation rate (in mm d^{-1}) for the sensitivity experiments with different stability weights on the moist adiabat below the freezing level in the Betts-Miller scheme: (a) $w = 0.7$ and (b) $w = 0.9$.

time scale becomes small, the model atmosphere is quickly adjusted toward a reference thermodynamic structure. On the other hand, the model atmosphere moves in the direction of the large-scale forcing when τ becomes large (Betts and Miller, 1986).

Figure 8 shows the zonally-averaged precipitation rate for the adjustment time scales of 1, 2 (control experiment) and 3 h. It is shown that the differences are small except for some portion of the tropical deep convection region. As the adjustment time scale increases, the maximum value in the zonally-averaged precipitation decreases. However, the difference between the maximum values in the simulations with $\tau = 1$ and 2 h is very small and in the region between 10°N and 25°N the simulation with $\tau = 2$ h produces more precipitation than that with $\tau = 1$ or 3 h. The geographical distribution of the precipitation rate simulated with different values of adjustment time scale is illustrated in Fig. 9 ($\tau = 1$ and 3 h) and Fig. 6a ($\tau = 2$ h). The spatial distribution pattern of the precipitation over Central Africa and Central America appears to be not

so sensitive to the adjustment time scale. However, significant differences between the simulated precipitation fields are observed over the tropical western Pacific where warm oceanic pool is present. The simulation with $\tau = 1$ h exhibits an intense precipitation zone centered near equator and 155°E, while the spatial distribution pattern in the simulation with $\tau = 3$ h somewhat resembles that in the AS simulation (Fig. 6b) in that it reveals two elongated precipitation areas. Over the Bay of Bengal and Burma, the localized precipitation becomes more excessively pronounced as the adjustment time scale becomes smaller. This is also true for the western Africa coastal region at ~ 10°N.

The first-guess reference temperature profile below the freezing level is established by assuming that the slope of the reference profile is some fraction w times that of a moist adiabat, that is,

$$\left(\frac{\partial\theta}{\partial p}\right)_{ref} = w\left(\frac{\partial\theta}{\partial p}\right)_{m}, \tag{3}$$

where θ is the potential temperature and p the pressure. The subscript m means that the quantity in parentheses is evaluated on a moist adiabat. From the freezing level to the cloud top, the first-guess temperature profile is constructed so that the thermal structure linearly (with respect to pressure height) approaches that of environment (model). The parameter w is called the stability weight on the moist adiabat below the freezing level. As the stability weight decreases below one, the reference thermal structure below the freezing level becomes more unstable than that of the moist adiabat. If the reference temperature profile exactly follows that on a moist virtual adiabat, which allows for buoyancy correction due to condensed cloud water, one can show that w at any pressure level is only a function of temperature and for a wide range of pressure and temperature its values are slightly greater that 0.9 (Betts, 1982; Baik *et al.*, 1991).

Figure 10 shows the zonally-averaged precipitation rate for the stability weights of 0.7, 0.8 (control experiment) and 0.9. As the stability weight increases, the zonally-averaged maximum precipitation associated with the tropical deep convection decreases. The geographical distribution of the precipitation rate simulated with different values of stability weight is presented in Fig. 11 ($w = 0.7$ and 0.9) and Fig. 6a ($w = 0.8$). Over Central Africa and Central America, the precipitation tends to increase as the stability weight decreases. The spatial distribution pattern of the precipitation over the tropical western Pacific is shown to be very sensitive to w, where unlike the north-southward elongated precipitation pattern in the simulation with $w = 0.8$ and the northwest-southeastward elongated precipitation pattern in the simulation with $w = 0.7$, the precipitation pattern in the simulation with $w = 0.9$ is prominently elongated east-westward

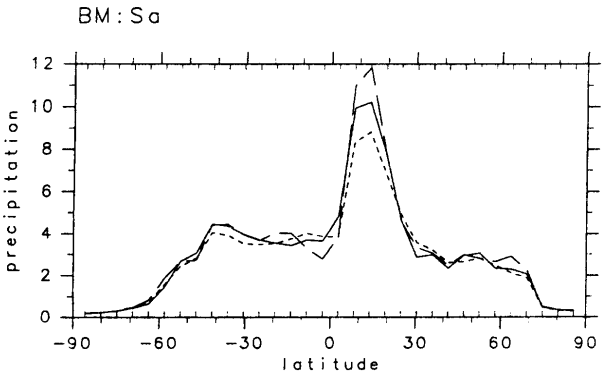

Fig. 12. Zonally-averaged total precipitation rate (in mm d^{-1}) for the sensitivity experiments with different saturation pressure departures at the lowest model prediction level in the Betts-Miller scheme. The short-dashed, solid and long-dashed lines correspond to $S_a = -20$, -30 and -40 mb, respectively.

The first-guess moisture profile is constructed using the saturation pressure departure parameter given by

$$S = p^* - p, \tag{4}$$

where p^* is the pressure at which an air parcel would become saturated if displaced dry-adiabatically from the pressure level of p. The saturation pressure departure is a measure of subsaturation, thus controlling relative humidity during the adjustment. The saturation pressure departure is assumed to linearly increase (in magnitude) to a value of $1.25S_a$ at the freezing level and then linearly decrease to $0.75S_a$ at the cloud top, where S_a represents the saturation pressure departure at the lowest model prediction level.

Figure 12 shows the sensitivity of the zonally-averaged precipitation rate to the saturation pressure departures of $S_a = -20$, -30 (control experiment) and -40 mb. As the saturation pressure departure increases (in magnitude), the precipitation increases over a wide area of tropical deep convection. This is because the convective precipitation is apt to take place in a less humid environment as the saturation pressure departure becomes larger (that is, threshold relative humidity becomes smaller). The difference in the zonally-averaged maximum precipitation rates between the experiments with $S_a = -20$ and -40 mb is as large as 3 mm d^{-1}. The geographical distribution of the precipitation rate simulated with different values of saturation pressure departure is illustrated in Fig. 13 ($S_a = -20$ and -40 mb) and Fig. 6a ($S_a = -30$ mb).

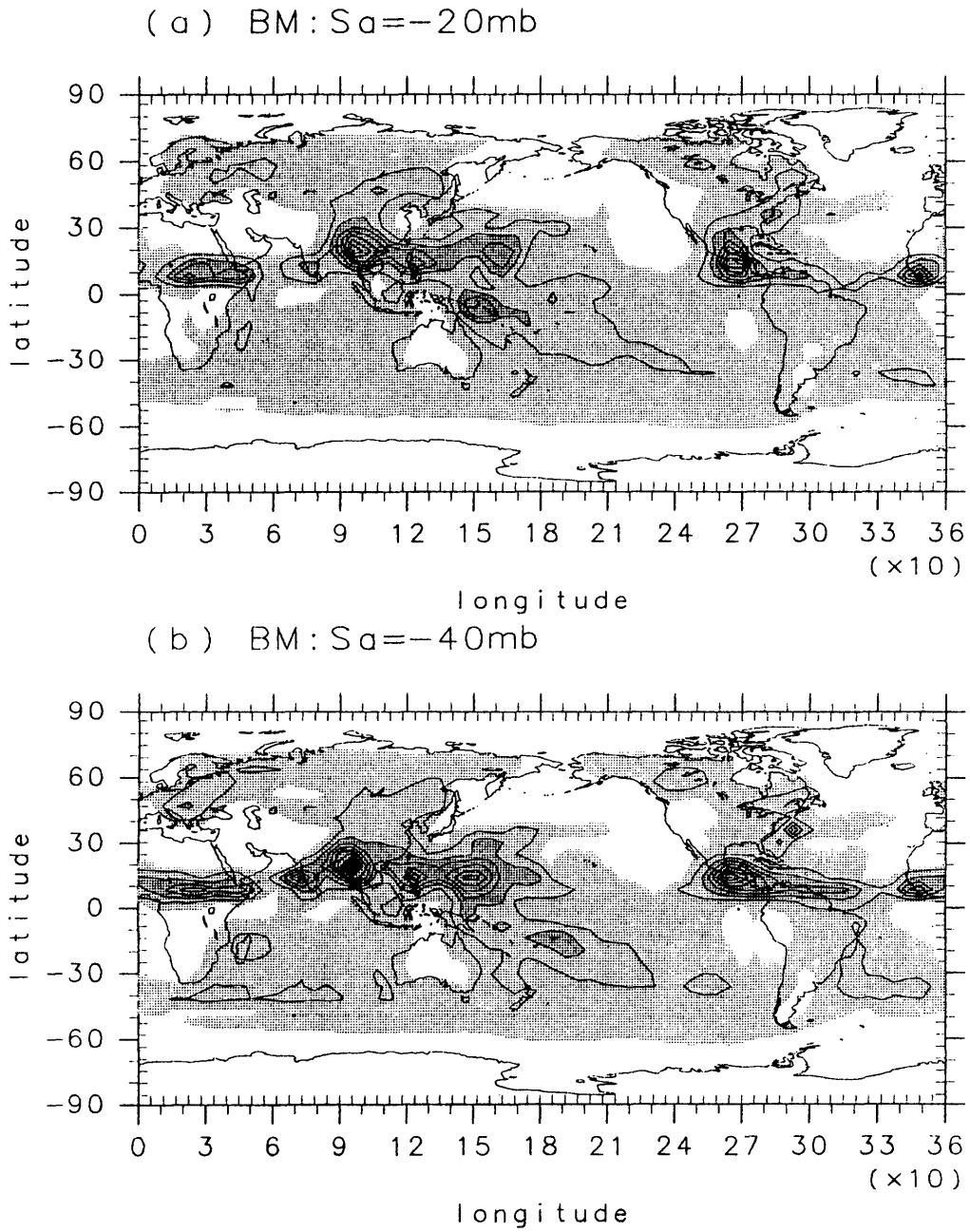

Fig. 13. Geographical distribution of the total precipitation rate (in mm d^{-1}) for the sensitivity experiments with different saturation pressure departures at the lowest model prediction level in the Betts-Miller scheme: (a) $S_a = -20$ mb and (b) $S_a = -40$ mb.

The simulation with $S_a = -40$ mb shows more intense precipitation over Central America with a farther extension into the central Atlantic than the simulation with $S_a = -20$ or -30 mb. Similar to the sensitivity results on the adjustment time scale and stability weight, the spatial distribution pattern of the precipitation over the tropical western Pacific is very sensitive to the saturation pressure departure. In the simulation with $S_a = -20$ mb there are a zonally-elongated precipitation zone at ~15°N and a small area of precipitation zone near the New Guinea, while in the simulation with $S_a = -40$ mb the precipitation is concentrated around ~15°N and ~150°E.

Using a limited-area model, Alapaty *et al.* (1994) investigated the sensitivity of orographic-convective rainfalls in the region of the western Ghats mountains and west coast of India during the southwest monsoon to the adjustment time scale and saturation pressure departure. Although the present model horizontal resolution is much coarser than that used by Alapaty *et al.* (1994), our result is

Table 2. The zonally-averaged convective, large-scale and total precipitation rates at a latitude where the zonally-averaged total precipitation is maximum in each sensitivity experiment using the Betts-Miller scheme, and the ratio of the zonally-averaged convective to total precipitation. Also, the results using the Arakawa-Schubert scheme are shown.

		convective precipitation (mm d^{-1})	large-scale precipitation (mm d^{-1})	total precipitation (mm d^{-1})	ratio (convective/ total)
adjustment time scale	$\tau = 1$ h	8.794	1.759	10.553	0.833
	$\tau = 2$ h	8.491	1.721	10.212	0.831
	$\tau = 3$ h	7.078	2.075	9.153	0.773
stability weight	$w = 0.7$	10.057	1.537	11.594	0.867
	$w = 0.8$	8.491	1.721	10.212	0.831
	$w = 0.9$	7.467	1.714	9.181	0.813
saturation pressure departure	$S_a = -20$ mb	6.590	2.230	8.820	0.747
	$S_a = -30$ mb	8.491	1.721	10.212	0.831
	$S_a = -40$ mb	10.405	1.433	11.838	0.879
Arakawa-Schubert scheme		8.929	1.272	10.201	0.875

consistent with theirs in a sense that the orographic-convective rainfall increases as the saturation pressure departure increases (Fig. 13 and Fig. 6a).

All the sensitivity experiments presented above show intense precipitation areas simulated over Central Africa, Central America and the Bay of Bengal and Burma, although the precipitation rate changes to some extent with changing adjustment parameters. Interestingly, the above sensitivity results indicate that over the tropical western Pacific the spatial distribution pattern of the precipitation is very sensitive to the adjustment time scale and stability weight as well as the saturation pressure departure. Also, in this region the spatial distribution pattern of the precipitation significantly depends on which cumulus parameterization scheme is employed (Fig. 6).

Recently, in an attempt to resolve the problems of occasionally producing heavy spurious precipitation over warm water and widely spread light precipitation over oceans in the NMC eta-model, Janjić (1994) introduced a cloud efficiency parameter to the Betts-Miller deep convection scheme. This parameter was introduced to take into account some dependence of the relaxation time scale and saturation pressure departure on different convective regimes. Although Janjić (1994) reported a considerable sensitivity to the choice of relative humidity profiles and the lower limit for the cloud efficiency, this approach seems to improve the original BM formulation since it allows for some degree of freedom in its application to convective regimes. The impact of the Janjić's formulation on the long-term GCM simulation needs to be investigated. However, the Janjić's formulation, in its essence, specifies the reference moisture profiles but with some degree of freedom, hence giving no guarantee for moisture predictability in a climate modeling.

In a limited-area, relatively high horizontal resolution model, it has been well recognized that interaction of the subgrid-scale latent heating with the grid-scale latent heating plays an important role in the dynamic and thermodynamic structure of the system (*e.g.*, Zhang and Fritsch, 1988). To get some insight into how the adjustment parameters in the BM scheme affect the partition between the convective and large-scale precipitations in the GCM with a coarse horizontal resolution, the ratio of the zonally-averaged convective to total precipitation is presented together with the zonally-averaged convective, large-scale and total precipitations in Table 2. The precipitation is zonally-averaged at a latitude where the zonally-averaged total precipitation is maximum in each sensitivity experiment using the BM scheme (*e.g.*, 13.8°N in the control simulation with $\tau = 2$ h, $w = 0.8$ and $S_a = -30$ mb). Also, the results using the Arakawa-Schubert scheme are presented in Table 2 for comparison.

Table 2 shows that as the adjustment time scale increases, the partition of the total precipitation into the large-scale precipitation (one minus the ratio given in the table) increases due to the gradual shift in the direction of the large-scale forcing. However, the difference in the ratios between the simulations with $\tau = 1$ and 2 h is very small. As the stability weight increases, the partition of the total precipitation into the convective precipitation decreases. As the saturation pressure departure becomes larger (in magnitude), the partition of the total precipitation into the large-scale precipitation becomes smaller since the convective precipitation is activated in a less humid environment, hence making the chance of the grid-scale supersaturation lower, for larger saturation pressure departure. Table 2 indicates that the partition between the convective and large-scale precipitations is most sensitive to the saturation pressure departure for the given ranges of the adjustment parameter values tested in this

study. Table 2 also indicates that the partition of the total precipitation into the convective precipitation in the AS scheme is generally larger than that in the BM scheme.

The results from Table 2 suggest that with changing adjustment parameter values interaction between the subgrid-scale latent heating and the large-scale latent heating as revealed by the partition ratios might be not so large due to a coarse horizontal resolution. This is contrasted with the results in the eta-model experiments by Janjić (1994). However, it should be noticed that since the large-scale condensation is used for the radiation calculation, a subtle change in the large-scale condensation can have a significant impact on the large-scale structures in a long-term GCM simulation through cloud-radiation interaction. For example, Table 2 shows that when the saturation pressure departure increases from -30 to -40 mb (in magnitude), the convective precipitation increases from 8.491 to 10.405 mm d^{-1}, but the large-scale precipitation decreases from 1.721 to 1.433 mm d^{-1}. This sensitiveness is somewhat demonstrated in the precipitation fields, especially over the tropical western Pacific (Figs. 6a, 9, 11 and 13).

5. Conclusion

Through a series of the GCM experiments, we emphasized that the precipitation distribution pattern over the tropical western Pacific, the most active convective region in the atmosphere, is very sensitive to the choice of cumulus parameterization and the convective adjustment parameters. It is also emphasized that among others in the Betts-Miller scheme the saturation pressure departure is the most sensitive parameter, which controls relative humidity. In a climate modeling, the realistic maintenance of long-term moisture structure is very important and this should be eventually connected with a cloud model for moisture predictability. The Arakawa-Schubert scheme consists of a closure assumption and a cloud model, while the Betts-Miller scheme does not have a cloud model, but specifies the moisture profile through the saturation pressure departure parameter. In this regard, the Arakawa-Schubert scheme, in principle, appears to be more suitable for a climate modeling than the Betts-Miller scheme, although the Betts-Miller scheme has shown remarkable skills in relatively short-term forecasts.

Acknowledgments

This research was performed while the first author was at the Center for Climate System Research, University of Tokyo as visiting associate professor. He would like to thank the University of Tokyo for providing associate professorship and Prof. Taroh Matsuno and other faculty and staff members for their sincere support during his stay. The authors would like to thank Mr. Toshiro Kumakura for helping prepare the model initial condition data and Dr. Atusi Numaguti for providing valuable comments on this study. The first author was supported by the Korea Ministry of Education through Grant for Research Institute in University.

References

Alapaty, K., R.V. Madala and S. Raman, 1994: Numerical simulation of orographic-convective rainfall with Kuo and Betts-Miller cumulus parameterization schemes. *J. Meteor. Soc. Japan*, **72**, 123–137.

Albrecht, B.A., V. Ramanathan and B.A. Boville, 1986: The effects of cumulus moisture transports on the simulation of climate with a general circulation model. *J. Atmos. Sci.*, **43**, 2443–2462.

Anthes, R.A., 1977: A cumulus parameterization scheme utilizing a one-dimensional cloud model. *Mon. Wea. Rev.*, **105**, 270–286.

Arakawa, A. and W.H. Schubert, 1974: Interaction of a cumulus cloud ensemble with the large-scale environment, Part I. *J. Atmos. Sci.*, **31**, 674–701.

Arakawa, A. and M.J. Suarez, 1983: Vertical differencing of the primitive equations in sigma coordinates. *Mon. Wea. Rev.*, **111**, 34–45.

Baik, J.-J., M. DeMaria and S. Raman, 1990a: Tropical cyclone simulations with the Betts convective adjustment scheme. Part I: Model description and control simulation. *Mon. Wea. Rev.*, **118**, 513–528.

Baik, J.-J., M. DeMaria and S. Raman, 1990b: Tropical cyclone simulations with the Betts convective adjustment scheme. Part II: Sensitivity experiments. *Mon. Wea. Rev.*, **118**, 529–541.

Baik, J.-J., M. DeMaria and S. Raman, 1991: Tropical cyclone simulations with the Betts convective adjustment scheme. Part III: Comparisons with the Kuo convective parameterization. *Mon. Wea. Rev.*, **119**, 2889–2899.

Betts, A.K., 1982: Saturation point analysis of moist convective overturning. *J. Atmos. Sci.*, **39**, 1484–1505.

Betts, A.K., 1986: A new convective adjustment scheme. Part I: Observational and theoretical basis. *Quart. J. Roy. Meteor. Soc.*, **112**, 677–691.

Betts, A.K. and M.J. Miller, 1986: A new convective adjustment scheme. Part II: Single column tests using GATE wave, BOMEX, ATEX and Arctic air-mass data sets. *Quart. J. Roy. Meteor. Soc.*, **112**, 693–709.

Betts, A.K. and M.J. Miller, 1993: The Betts-Miller scheme. *The Representation of Cumulus Convection in Numerical Models, Meteor. Monogr.* No. 46, Amer. Meteor. Soc., 107–121.

Cheng, M.-D. and A. Arakawa, 1990: Inclusion of convective downdrafts in the Arakawa-Schubert cumulus parameterization. Tech. Rep., Dept. of Atmospheric Sciences, University of California at Los Angeles, 69 pp.

Chou, M.-D., 1992: A solar radiation model for use in climate studies. *J. Atmos. Sci.*, **49**, 762–772.

Cunnington, W.M. and J.F.B. Mitchell, 1990: On the dependence of climate sensitivity on convective parameterization. *Climate Dynamics*, **4**, 85–93.

Evans, J.L., B.F. Ryan and J.L. McGregor, 1994: A numerical exploration of the sensitivity of tropical cyclone rainfall intensity to sea surface temperature. *J. Climate*, **7**, 616–623.

Hack, J.J., 1994: Parameterization of moist convection in the National Center for Atmospheric Research community climate model (CCM2). *J. Geophys. Res.*, **99**, 5551–5568.

Janjić, Z.I., 1990: The step-mountain coordinate: Physical package. *Mon. Wea. Rev.*, **118**, 1429–1443.

Janjić, Z.I., 1994: The step-mountain eta coordinate model: Further developments of the convection, viscous sublayer, and turbulence closure schemes. *Mon. Wea. Rev.*, **122**, 927–945.

Kondo, J., 1993: A new bucket model for predicting water content in the surface soil layer. *J. Japan Soc. Hydrol. Water Res.*, **6**, 344–349. (in Japanese)

Kuo, H.L., 1965: On formation and intensification of tropical cyclones through latent heat release by cumulus convection. *J. Atmos. Sci.*, **22**, 40–63.

Kuo, H.L., 1974: Further studies of the parameterization of the influence of cumulus convection on large-scale flow. *J. Atmos. Sci.*, **31**, 1232–1240.

Le Treut, H. and Z.-X. Li, 1991: Sensitivity of an atmospheric general circulation model to prescribed SST changes: Feedback effects associated with the simulation of cloud optical properties. *Climate Dynamics*, **5**, 175–187.

Louis, J., 1979: A parametric model of vertical eddy fluxes in the atmosphere. *Bound. Layer Meteor.*, **17**, 187–202.

Manabe, S. and D.G. Hahn, 1981: Simulation of atmospheric variability. *Mon. Wea. Rev.*, **109**, 2260–2286.

Manabe, S., J. Smagorinski and R.F. Strickler, 1965: Simulated climatology of a general circulation model with a hydrologic cycle. *Mon. Wea. Rev.*, **93**, 769–798.

McFarlane, N.A., 1987: The effect of orographically excited gravity wave drag on the general circulation of the lower stratosphere and troposphere. *J. Atmos. Sci.*, **44**, 1775–1800.

Mellor, G.L. and T. Yamada, 1974: A hierarchy of turbulence closure models for planetary boundary layers. *J. Atmos. Sci.*, **31**, 1791–1806.

Mellor, G.L. and T. Yamada, 1982: Development of a turbulence closure model for geophysical fluid problems. *Rev. Geophys. Space Phys.*, **20**, 851–875.

Miller, M.J., A.C.M. Beljaars and T.N. Palmer, 1992: The sensitivity of the ECMWF model to the parameterization of evaporation from the tropical oceans. *J. Climate*, **5**, 418–434.

Nakajima, T. and M. Tanaka, 1986: Matrix formulation for the transfer of solar radiation in a plane-parallel scattering atmosphere. *J. Quant. Spectrosc. Radiat. Transfer*, **35**, 13–21.

Numaguti, A., 1993: Dynamics and energy balance of the Hadley circulation and the tropical precipitation zones: Significance of the distribution of evaporation. *J. Atmos. Sci.*, **50**, 1874–1887.

Numaguti, A. and T. Kumakura, 1994: A user's guide to the CCSR/NIES atmospheric general circulation model (version 5.3), 42 pp. (in Japanese)

Numaguti, A., S. Sugata, S. Mitsumoto, M. Takahashi, M. Kimoto, T. Nakajima, A. Sumi and T. Matsuno, 1994: Current status of CCSR/NIES atmospheric general circulation model. UCLA/University of Tokyo Joint Workshop, Tokyo, Abstracts, 33.

Pitcher, E.J., R.C. Malone, V. Ramanathan, M.L. Blackmon, K. Puri and W. Bourke, 1983: January and July simulations with a spectral general circulation model. *J. Atmos. Sci.*, **40**, 580–604.

Puri, K. and M.J. Miller, 1990: Sensitivity of ECMWF analyses-forecasts of tropical cyclones to cumulus parameterization. *Mon. Wea. Rev.*, **118**, 1709–1741.

Slingo, A., R.C. Wilderspin and R.N.B. Smith, 1989: Effect of improved physical parameterizations on simulations of cloudiness and the earth's radiation budget. *J. Geophys. Res.*, **94**, 2281–2301.

Takahashi, M., 1993: A QBO-like oscillation in a two-dimensional model derived from a GCM. *J. Meteor. Soc. Japan*, **71**, 641–654.

Tiedtke, M., 1988: Parameterization of cumulus convection in large-scale models. *Physically-Based Modelling and Simulation of Climate and Climatic Change — Part I*, Kluwer Academic Publishers, 375–431.

Tiedtke, M., 1989: A comprehensive mass flux scheme for cumulus parameterization in large-scale models. *Mon. Wea. Rev.*, **117**, 1779–1800.

Zhang, D.-L. and J.M. Fritsch, 1988: Numerical sensitivity experiments of varying model physics on the structure, evolution and dynamics of two mesoscale convective systems. *J. Atmos. Sci.*, **45**, 261–293.

2つの積雲対流パラメタリゼーションのGCMによる感応実験

Jong-Jin Baik[1,2]・高橋正明
（東京大学気候システム研究センター）

Betts-MillerとArakawa-Schubertの積雲対流パラメタリゼーションの感応実験を実行した。水平分解能T21、鉛直20層のCCSR/NIES大気大循環モデルを用いて、一連の6カ月積分を行い、最後の3カ月、6–8月の時間平均値で比較を行った。再現された大規模場の構造はだいたい似ているが、いくつかの注目すべき違いが存在する。それは、北半球中緯度の中・上層の温度、熱帯対流域の対流による最大熱源の位置、境界層での熱源/冷源、熱帯西太平洋の降水パターン、乱流による熱輸送の鉛直分布である。Betts-Millerスキームのパラメタ実験では、熱帯西太平洋の降水パターンが飽和圧力差のみでなく緩和時間や安定度に非常に敏感である。また対流による降水と大規模凝結による降水の比率は飽和圧力差にもっとも敏感であることも示される。

[1]Global Environment Laboratory, Yonsei University, Seoul, Koreaより滞在中
[2]現在所属：Department of Environmental Science and Engineering, Kwangju Institute of Science and Technology, Kwangju, Korea